Water Air Soil Pollut (2013) 224:1569
DOI 10.1007/s11270-013-1569-2

The Applications of Lithium Zirconium Silicate at High Temperature for the Carbon Dioxide Sorption and Conversion to Syn-gas

Reshma Raskar · Vilas Rane · Abaji Gaikwad

Received: 29 November 2012 / Accepted: 10 April 2013 / Published online: 15 May 2013

Abstract The applications of different samples of lithium zirconium silicate contributing to CO_2 sorption and conversion of CO_2 to syn-gas at high temperatures were investigated. Several samples of lithium zirconium silicate prepared by solid–solid fusion method were calcined in air or nitrogen atmosphere at 900 °C for 3 h. The lithium zirconium silicate samples were characterized by acidity/alkalinity, surface area, XRD pattern, SEM images, and CO_2 sorption. The alkalinity and surface area of the samples of lithium zirconium silicate were found to be in the range of 15.1 to 20.0 mmol g^{-1} and 0.05 to 2.13 m^2 g^{-1}, respectively. The temperature profile of CO_2 sorption by samples of lithium zirconium silicate was given for the range 100 to 700 °C. The CO_2 sorption was found to be in the range of 12.81 to 18.04 wt.% at 550 °C for samples of lithium zirconium silicate with different Li/Zr/Si mole ratios from 1 to 6. The crystalline phases in the samples of the lithium zirconium silicate, $Li_6Si_2O_7$, $ZrSiO_4$, Li_2SiO_3, Li_2ZrO_3, Li_4ZrO_4, and Li_4SiO_4 could contribute to CO_2 capture. The conversion of CO_2 by methane to syn-gas over the lithium silicate samples and PdO (5 wt.%)/Al_2O_3 at 500 °C with the gas hourly space velocities 6,000, 12,000, and 36,000 mL h^{-1} g^{-1} of methane and 6,000 mL h^{-1} g^{-1} of CO_2 was explored. However, the higher conversion of CO_2 to syn-gas was observed at the low gas hourly space velocity of 6,000 mL h^{-1} g^{-1} of methane.

R. Raskar · V. Rane · A. Gaikwad (✉)
CE and PD Division, National Chemical Laboratory,
Pune 411 008, India
e-mail: ag.gaikwad@ncl.res.in

Keywords CO_2 sorption · Applications of lithium zirconium silicate · Solid–solid fusion method · Temperature profile · Syn-gas

1 Introduction

Due to the high thermal stability and low activity of CO_2, to achieve the conversion of CO_2 to a single value-added product through a single step seems to be a tough task. However, there is a possibility that CO_2 can be converted to a value-added product through intermediate products (Graves et al. 2011). Therefore, here, as a first step process towards value-added products, an attempt has been made to improve CO_2 sorption by an adsorbent and then to convert the adsorbed CO_2 to syn-gas, and then, the second step is to convert the syn-gas to hydrocarbons or value-added products (Yin et al. 2013).

In the present environment scenario, large amounts of emitted gases such as sulfur dioxide, nitrous oxide, carbon monoxide, and methane are causing air and water pollution in excess of the tolerance limit. The excess acidic gas concentrations in the atmosphere also cause acid rain and global warming. The main sources of carbon dioxide are fossil fuel combustion, aircraft, vehicles, refineries, and natural gas combustion centers. From the free- to post-industrial area, the CO_2 concentration in the atmosphere has increased from 250 to 391 ppm. Therefore, the capture, sequestration, and utilization of greenhouse gases are the important issues to be addressed by investigating new concepts and processes (NOAA 2012; Etheridge

et al. 1996). The captured CO_2 by the adsorbent involved the adsorption of CO_2 on the surface, in the pores (by capillary action), and carbonate formation. The captured CO_2 by the amines and ionic liquids is a slow kinetic reaction. Carbon, zeolites, amines, and ionic liquids are not suitable adsorbents for CO_2 due to a decline in their capturing capacity at high temperatures (>450 °C) (Stuckert and Yang 2011; Chatti et al. 2009). The captured CO_2 by the mixed metal oxides at higher temperatures involved carbonate formation and adsorption in the pores and on the surface. The mixed metal oxides are thermally stable at post- and pre-combustion temperatures. The alkali and alkaline earth metal oxides form carbonates by reacting with CO_2. The CO_2 capture by carbonate formation of mixed metal oxide with CO_2 is a reversible and non-polluting process (Fauth et al. 2004; Pfeiffer et al. 2007). Therefore, mixed metal oxides are good candidates for the capture of CO_2 at high temperatures, 500 to 1,000 °C. Mainly, magnesium, calcium, and lithium containing aluminates, zirconate or silicate, or transition metal oxides have been explored for the capture of CO_2. The reaction of CO_2 with magnesium aluminum hydrotalcite (Hutson and Attwood 2008; Yong et al. 2001; Nakagawa et al. 2003; Iwan et al. 2009) was explored in the temperature range 150 to 500 °C. The reaction of carbon dioxide with lithium containing the mixed metal oxides was studied in the temperature range 40 to 700 °C. The equilibrium and kinetics of the reaction of carbon dioxide with lithium zirconate were explored (Ida and Lin 2003; Mosqueda et al. 2006; Gupta and Fan 2002; Avalos-Rendon et al. 2009; Khomane et al. 2006; Wang and Lee 2009; Pfeiffer and Bosch 2005; Yi and Eriksen 2006; Kalinkin et al. 2003; Nakagawa et al. 2003; Iwan et al. 2009) at temperature range 400 to 700 °C. Promoter effect of potassium and lithium by adding in lithium zirconate showed an enhanced reaction of carbon dioxide with lithium zirconate (Kalinkin et al. 2003; Nakagawa et al. 2003; Iwan et al. 2009; Ida and Lin 2003; Ochoa-Fernandez et al. 2006a, b; Fauth et al. 2005; Ide et al. 2005; Minghua et al. 2008).

The formation of different phases, Li_2ZrO_3, Li_4ZrO_4, etc., of lithium zirconate based on the Li/Zr mole ratio had been reported (Hellstrom and Van Gool 1981). The enthalpies for the formation of different phases of lithium zirconium were reported, Li_2ZrO_3 ($-1{,}742.8$ kJ mol^{-1}) < Li_4ZrO_4 < $Li_6Zr_2O_7$ ($-4{,}107.1$ kJ mol^{-1}) < Li_8ZrO_6 ($-3{,}559.7$ kJ mol^{-1}) (Wyers et al. 1989). The preparation of Li_4SiO_4 silicate phases had been confirmed by X-ray diffraction (XRD) pattern, and the formation of polygonal particles of the Li_4SiO_4 silicate phases were observed by scanning electron microscope (SEM) images (Venegas et al. 2007). The thermal stability of zircon ($ZrSiO_4$) had been reported with the confirmation of a particle with a blocky shape of the original grits by SEM images and the formation of crystalline zircon ($ZrSiO_4$) phase by the XRD pattern (Kaiser et al. 2008). The preparation, characterization, and ion exchange properties of lithium zirconium silicate had been reported (El-Naggar and Abou-Mesalam 2006). The preparation and characterization of the iron containing the red glass pigment of lithium zirconium silicate with their different phases had been reported (Bondioli et al. 2004). The characterization had been reported of natural lithium sodium zirconium silicate (Dunn et al. 1977). However, the multi-component mixed metal oxides such as calcium copper titanate, lithium zirconium silicate, calcium copper lanthanide, calcium zirconium silicate, etc. had not been explored for CO_2 capture.

The conversion and utilization of methane and carbon dioxide are the important issues in the context of global warming effect from the two greenhouse gases. The plasma catalytic activation of methane and carbon dioxide was investigated for syn-gas production (Zhang et al. 2010). The 3 % Ru-Al_2O_3 and 2 % Rh-CeO_2 catalysts were synthesized and tested for CH_4–CO_2 reforming activity using either CO_2-rich or CO_2-lean model biogas feed (Djinovi et al. 2011). A thermodynamic equilibrium analysis on the multi-reaction system for carbon dioxide reforming of methane in view of carbon formation was reported with aspen plus based on the direct minimization of the Gibbs free energy method. The effects of CO_2/CH_4 ratio (0.5–3), reaction temperature (300–1,200 °C), and pressure (1–25 atm) on equilibrium conversions, product compositions, and solid carbon were explored (Nikoo and Amin 2011). MgO–ZrO_2 mesoporous support (Zr/Mg molar ratio=9) impregnated with 6 wt.% Ni, 6 wt.% Co, and 3 wt.% of both Ni and Co prepared by a novel surfactant-assisted impregnation method was used for carbon dioxide reformation of methane at a CH_4/CO_2 feed ratio of 1,750 °C, 1 atm with a gas hourly space velocity of 125,000 mL g^{-1} h^{-1} (Fan et al. 2010). A review reported the opportunities and prospects in the chemical recycling of carbon dioxide to fuels, as a

coming technology to carbon sequestration and storage (Centi and Perathoner 2010). The reformation of CH_4 with CO_2 or steam produced synthesis gas. Although, these two reactions have similar thermodynamic characteristics, there is a greater potential for carbon formation (Edwards and Maitra 1995). CuFe-based CuFeMg-layered double hydroxide catalyst showed good activity and selectivity towards catalytic conversion of syn-gas to mixed alcohols (Gao et al. 2013). The review described the different catalytic options for the production of syn-gas and hydrogen from the hydrogen-containing molecules (Pen et al. 1996). Thus, the mixed metal oxides have been used to capture the CO_2 or convert the CO_2 by methane to syn-gas. The uses of mixed metal oxides for the capture CO_2 and then their application to conversion into syn-gas are lacking. Therefore, this paper reports the sorption of CO_2 by the samples of lithium zirconium silicate and also the CO_2 conversion to syn-gas by methane over the lithium zirconium silicate and PdO (5 wt.%)/Al_2O_3 at higher temperatures.

2 Methods

2.1 Reagents and Apparatus

The chemicals lithium and zirconium carbonate, fumed SiO_2 (Sigma-Aldrich), were used for the preparation of samples of the lithium zirconium silicate. All chemicals used were of analytical grade. The alumina-supported palladium (Pd (5 wt.%)/Al_2O_3) was used for the CO_2 conversion by methane reaction (Lancaster chemicals) after calcinations at 600 °C for 3 h. The high-purity gases carbon dioxide and helium were used (Deluxe India, Ltd.). A high-temperature furnace was used to calcine the samples of the lithium zirconium silicate (Thermax Co., Ltd.). A split furnace (Carbolite USA) was used to carry the reaction of carbon dioxide with the samples of the lithium zirconium silicate at different temperatures. GC (Nucon India, Ltd.) with thermal conductivity detector was used to analyze the carbon dioxide.

2.2 Procedure for Preparation of Samples of the Lithium Zirconium Silicate

Samples of the lithium zirconium silicate were prepared by solid–solid fusion method for the different Li/Zr/Si mole ratios. While preparing the samples of the lithium zirconium silicate with Li/Zr/Si (6:1:1) mole ratio, 0.072 mol of lithium carbonate, 0.012 mol of each zirconium carbonate, and fumed SiO_2 were used. The solid mass was thoroughly mixed and then calcined at 900 °C for 3 h. The particles −22 to −30 mesh sizes used for gas–solid reaction were prepared from the calcined solid mass. The samples of the lithium zirconate, lithium silicate zirconium silicate, and lithium zirconium silicate, henceforth are indicated by the terminology taking into account the first letter of the name of the metal element, and the metal mole ratio, such as, LZ61 for Li/Zr (6:1), LS61 for Li/Si (6:1), ZS11 for Zr/Si (1:1), LZS111 for Li/Zr/Si (1:1:1), LZS311 for Li/Zr/Si (3:1:1), LZS411 for Li/Zr/Si (4:1:1), and LZS611 for Li/Zr/Si (6:1:1). The alumina-supported palladium (Pd (5 wt.%)/Al_2O_3) used for the CO_2 conversion by methane was calcined at 600 °C in air for 3 h.

2.3 Characterizations of the Samples of the Lithium Zirconium Silicate

The samples of the lithium zirconium silicate were characterized for the alkalinity/acidity, XRD patterns (Philips Power XRD), FTIR (Perkin Elmer Spectrum I), the surface area (model Autosorb-1, Make-Quantachrome Instruments Pvt. Ltd., USA), and SEM images (QUANTA 200 3D).

2.4 Procedure for CO_2 Sorption

An online setup of gaseous connection was used for the reaction of carbon dioxide with the samples of lithium zirconium silicate. The setup was developed by using a 4-mm outer diameter (od) stainless steel tubing, four three-way gas valves, gas sampling valve, carbolite split furnace with temperature controller, a quartz reactor, Nucon GC, and gas flow control valves. The flow rates of helium and carbon dioxide gases were changed with four three-way gas valves as required, as shown in Fig. 1a. A quartz tube reactor was prepared by using a quartz tube with the dimensions 6-mm od, 4-mm inner diameter (id), and 850-mm length. The quartz tube reactor was modified at the center by using a quartz tube with the dimensions 10 to 20 mm id and 100-mm length. The sample of the lithium zirconium silicate was placed inside and at the center of a quartz tube reactor with the support of a quartz

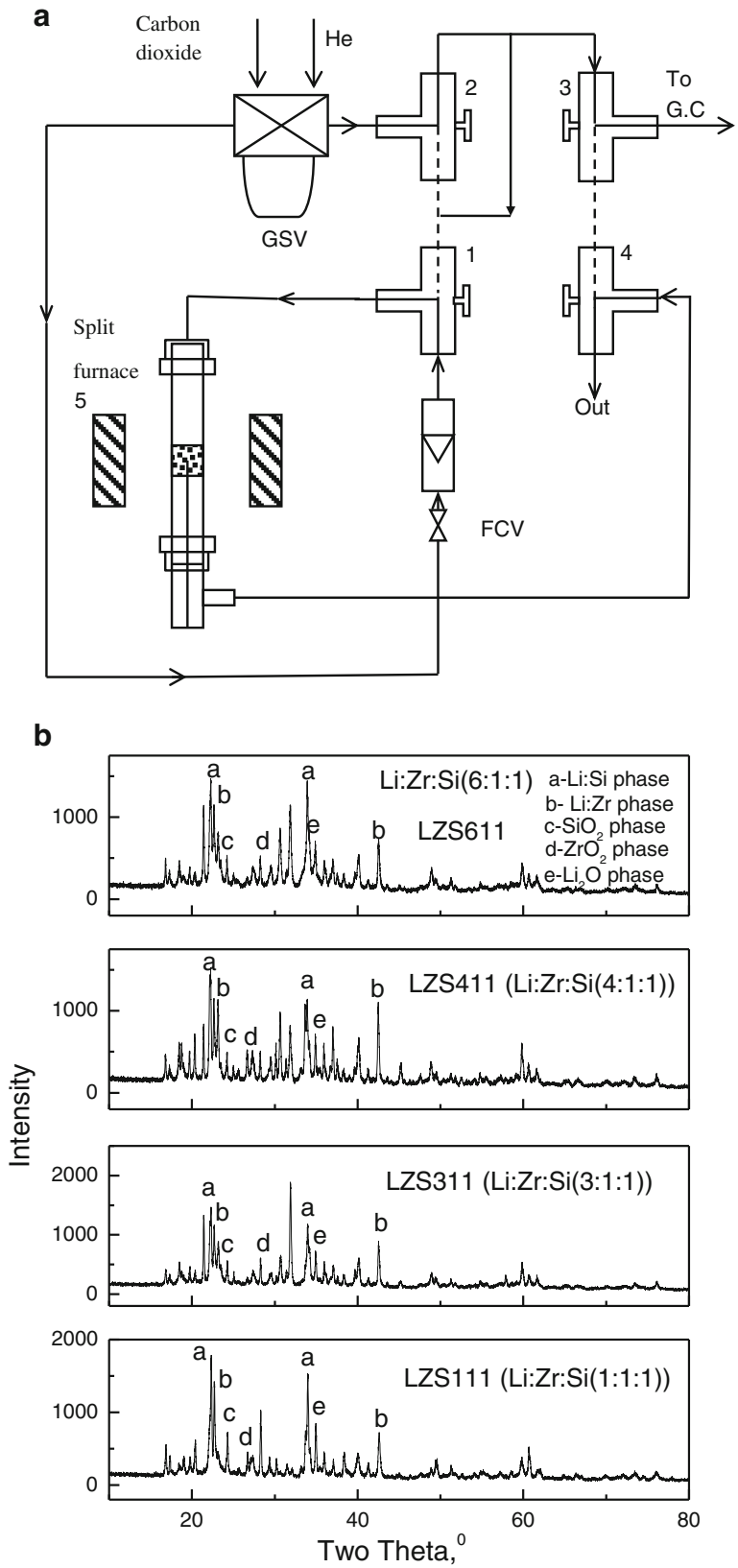

Fig. 1 **a** The systematic presentation of fixed bed reactor for the CO_2 sorption and conversion to syn-gas. **b** The XRD pattern of the lithium zirconium silicate samples, LZS611 (Li/Zr/Si, 6:1:1), LZS411 (Li/Zr/Si, 4:1:1), LZS311 (Li/Zr/Si, 3:1:1), and LZS111 (Li/Zr/Si, 1:1:1) were prepared by the solid–solid fusion method

wool. The quartz reactor was placed inside a split furnace. The temperature of the split furnace was controlled by a temperature controller. The temperature of the sample of the lithium zirconium silicate was measured by using a thermocouple and temperature indicator. The quartz reactor was connected through four three-way gas valves and a gas sampling valve to GC by using stainless steel tubing connections. Of the sample of lithium zirconium silicate, 0.05 to 0.1 g with particle size −22 to −30 meshes was used to react with CO_2. First, the sample of the lithium zirconium silicate was flushed with helium gas in order to remove the stresses of other gases. Then, the sample of the lithium zirconium silicate bed was flushed with CO_2 to remove the free helium gas. After that, the carbon dioxide was allowed to react with the sample of the lithium zirconium silicate in the absence of helium at a certain pressure, temperature, and time. Then, the reacted carbon dioxide with the sample of the lithium zirconium silicate was removed by using helium as a carrier gas, and increasing the temperature of the sample of the lithium zirconium silicate bed to 900 °C. The removed carbon dioxide was analyzed by GC using a Porapak-Q column and a thermal conductivity detector. The adsorbed carbon dioxide by the sample of the lithium zirconium silicate was expressed as weight percent of CO_2 at STP. There were two peaks observed (Hutson and Attwood 2008). The first peak represented the physic-sorption of weakly bound CO_2. The second peak represented the chemisorptions of strongly bound CO_2.

2.5 Procedure for Conversion of CO_2 to Syn-gas

The reactions of carbon dioxide and methane were carried in the fixed bed quartz reactor. The system used was the same as described above, but the system was set by changing the ways of gas through the three-way gas valves. The temperature of the catalyst bed of lithium zirconium silicate or alumina-supported palladium oxide in the fixed bed reactor, with helium as carrier gas, was set at a particular temperature with a temperature controller. Then the reacting gas mixture was introduced in the helium carrier gas in order to pass the reaction mixture through the catalyst bed. The outlet reacted gas mixture was analyzed by pulse method by using the gas sampling valve connected to the on line system to the GC with TCD and FID detectors. The results were reported here of conversion of CO_2 and methane and the selectivity to CO.

3 Results and Discussions

The carbonate formation reactions could be given by following equations.

$$Li_2ZrO_3 + CO_2 \leftrightarrow ZrO_2 + Li_2CO_3 \quad (1)$$

$$Li_2SiO_3 + CO_2 \leftrightarrow SiO_2 + Li_2CO_3 \quad (2)$$

$$Li_4SiO_4 + 2CO_2 \leftrightarrow 2Li_2CO_3 + SiO_2 \quad (3)$$

$$ZrO_2 + CO_2 \rightarrow ZrOCO_3 \quad (4)$$

$$Li_6Zr_2O_7 + 3CO_2 \leftrightarrow 3Li_2CO_3 + 2ZrO_2 \quad (5)$$

$$M^{(n-1)+} - OH + CO_2 \leftrightarrow M^{(n-1)+} - HCO_3 \quad (6)$$

$$M^{n+} \leftarrow H_2O + CO_2 \leftrightarrow M^{n+} \leftarrow H_2CO_3, \quad (7)$$

where, M^{n+} stands for the metal ion in the mixed metal oxides. Thus, several reactions are occurring simultaneously and reversibly could help capture and release the CO_2 during the reactions. The hydroxyl groups and water molecules attached to the metal ions depend on the calcination, pre-treatment, and activation temperatures before the use of an adsorbent to applications (Hutson and Attwood 2008).

The reactions of CO_2 with methane for the syn-gas formation could be given as

$$CO_2(\text{at high mole ratio}) + CH_4(\text{at low mole ratio}) \leftrightarrow 2CO + 2H_2 \quad (8)$$

3.1 Characterization of the Samples of Lithium Zirconium Silicate

The samples of lithium zirconium silicate had been characterized for the surface area, alkalinity/acidity, SEM images, and XRD patterns. In Fig. 1b, the represented XRD patterns of the samples LZS611, LZS411, LZS311, and LZS111 of lithium zirconium silicate were prepared by the solid–solid fusion method with the different mole ratios (Li/Zr/Si, 6:1:1, 4:1:1, 3:1:1, and

1:1:1). The phases of the Li_2O, ZrO_2, SiO_2, lithium zirconate, lithium silicate, zirconium silicate, and lithium zirconium silicate were observed (Fig. 1b). However, the crystalline phases of the $Li_6Si_2O_7$, Li_2SiO_3, Li_2ZrO_3, Li_4ZrO_4, Li_4SiO_4, and $ZrSiO_4$ were predominantly seen in the samples LZS611, LZS411, and LZS311 when the Li/Zr/Si, 6:1:1, 4:1:1, and 3:1:1 mole ratios were used while preparing the samples of lithium zirconium silicate. However, lithium-rich phases in the samples of lithium zirconate and lithium silicate were not observed when the sample LZS111 (Li/Zr/Si, 1:1:1 mole ratios) was characterized.

In Fig. 2a, the XRD patterns of sample LZS611 of lithium zirconium silicate with Li/Zr/Si, 6:1:1 mole ratio, the sample LZ61 of lithium zirconate with Li/Zr, 6:1 mole ratio, the sample LS61 of lithium silicate with Li/Si, 6:1 mole ratio and the sample ZS11 of zirconium silicate with Zr/Si, 1:1 mole ratio were given. However, the crystalline phases of the lithium zirconate Li_4ZrO_4, Li_2ZrO_3 and lithium silicate, Li_2SiO_3, Li_4SiO_4 were predominantly seen in the samples LZ61 and LS61 of lithium zirconium and lithium silicate, respectively. Moreover, the zirconium silicate phase $ZrSiO_4$ was predominantly observed in the sample ZS11of zirconium silicate with Zr/Si, 1:1 mole ratio.

In Fig. 2b, the infrared spectroscopy (IR) of the samples of the lithium zirconate, lithium silicate, and zirconium silicate was plotted by using the intensity versus the wave numbers from 450 to 4,000 cm^{-1} in order to check the phase formation by bonding of metal–metal through oxygen. The results indicate that as the content of lithium in the samples of lithium zirconate and lithium silicate changes, the different phase formations through the interlinking through bonding of oxygen, lithium, zirconium, and silicon were observed from wave numbers 450 to 4,000 cm^{-1}. The bonding between metal and oxygen for the metal crystalline phases though ZrO_a^{2-a} and SiO_b^{2-b} was observed for wave numbers 450 to 2,000 cm^{-1}. However, the bonding of water molecules to metal was observed in between wave numbers 3,000 and 4,000 cm^{-1}. The bonded water molecules to metal could help capture CO_2 by forming carbonate ions.

In Fig. 2c, the IR of the samples of lithium zirconium silicate was given in order to see the phase formation. The IR of intensity versus the wave numbers from 450 to 4,000 cm^{-1} was given. The results indicate that as the mole ratio of lithium in the samples of lithium zirconium silicate increases from 1 to 6, the different phase formations through the interlinking through bonding the oxygen, lithium, zirconium, and silicon were observed from wave numbers 450 to 4,000 cm^{-1}. The bonding between metal and oxygen is observed for wave numbers 450 to 2,000 cm^{-1}. However, the bonding of water molecules to the metal was observed in between wave numbers 3,000 and 4,000 cm^{-1}. The bonded water molecules to metal help capture CO_2 by forming carbonate ions.

In Table 1, the surface areas and alkalinity of the different samples of lithium zirconium silicate were given. Sample LZ61 of lithium zirconate with mole ratio Li/Zr, 6:1, the sample LS61 of lithium silicate with mole ratio Li/Si, 6:1, and the sample ZS11 of zirconium silicate with mole ratio Zr/Si, 1:1 showed the surface area, 3.36, 6.94, and 98.71 $m^2\ g^{-1}$, respectively. The metal content, method of preparation, calcination temperature, crystalline phase, pore formation, etc. contribute to the surface area. However, the sample SZ11 of zirconium silicate with mole ratio Zr/Si, 1:1 had the higher surface area. That indicates that the sample zirconium silicate is a more porous material.

The samples LZS111, LZS311, LZS411, and LZS611 of lithium zirconium silicate with mole ratios Li/Zr/Si, 1:1:1, 3:1:1, 4:1:1, 6:1:1 had surface areas of 0.05, 0.16, 1.43, and 2.13 $m^2\ g^{-1}$, respectively. The results indicate that the samples of lithium zirconium silicate are less porous materials. The surface area of the samples of lithium zirconium silicate was varied from 0.05 to 2.13 $m^2\ g^{-1}$ by increasing the mole ratio of lithium from 1 to 6.

The sample LZ61 of lithium zirconate with mole ratio Li/Zr, 6:1, the sample of LS61 lithium silicate with mole ratio Li/Si, 6:1 and the sample ZS11 of zirconium silicate with mole ratio Zr/Si, 1:1 had shown 21.25 (alkalinity), 21.34 (alkalinity), and 0.23 mmol g^{-1} (acidity), respectively. These results indicate that the lithium content in these samples had significantly increased the alkalinity by forming the mixed metal oxides, lithium zirconate, and silicate phases. However, the sample of zirconium silicate had shown the acidity 0.23 mmol g^{-1}. The results had shown that both zirconium and silicon had contributed to the acidity by forming the mixed metal oxide and zirconium silicate phases.

The samples LZS111, LZS311, LZS411, and LZS611 of the lithium zirconium silicate with mole ratios Li/Zr/Si, 1:1:1, 3:1:1, 4:1:1, 6:1:1 had shown the

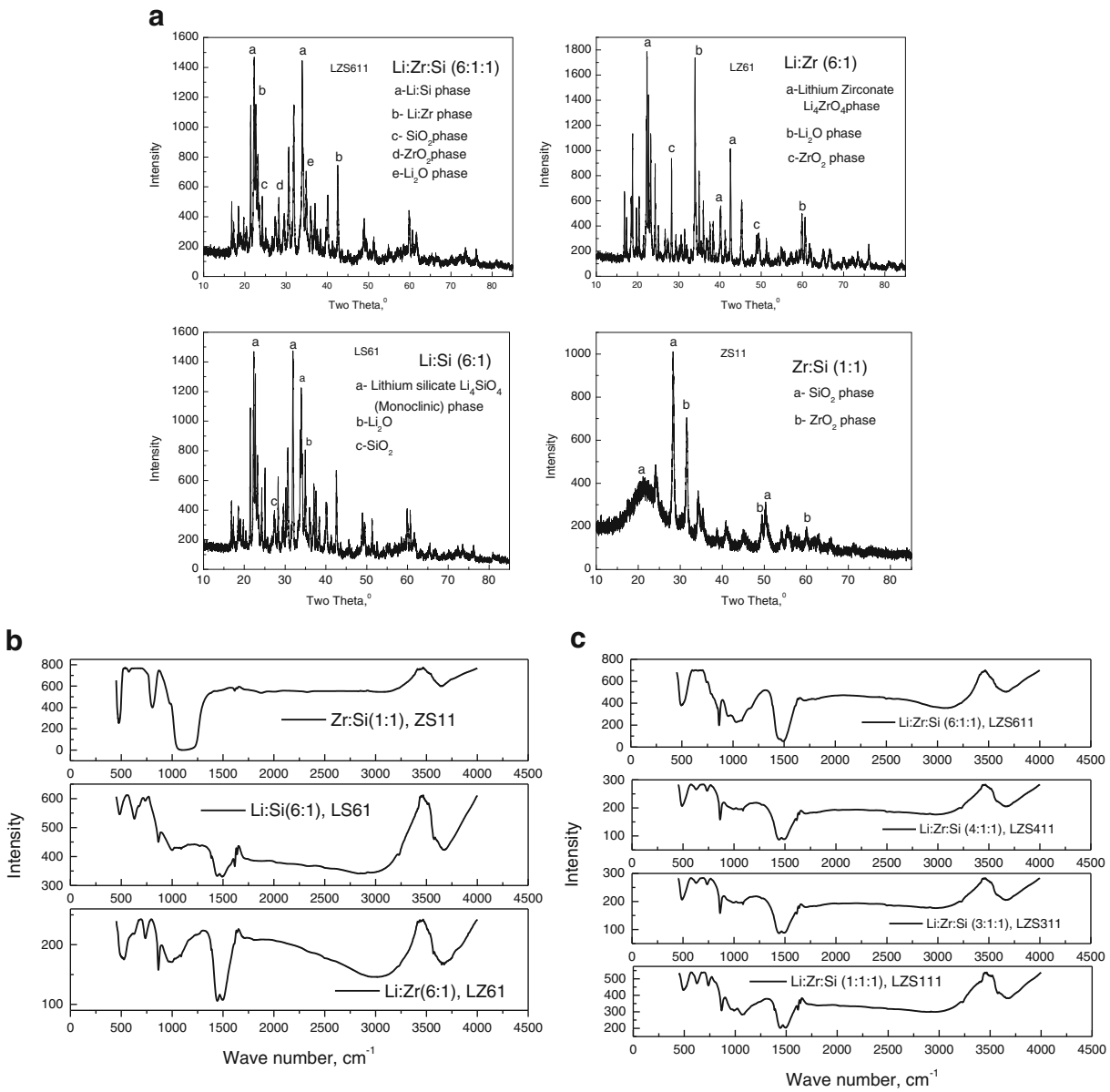

Fig. 2 **a** The XRD pattern of the lithium zirconium silicate, lithium zirconate, lithium silicate, and zirconium silicate samples, LZS611 (Li/Zr/Si, 6:1:1), LZ61 (Li/Zr, 6:1), LS61 (Li/Si, 6:1), and ZS111 (Zr/Si, 1:1) were prepared by the solid–solid fusion method. **b** The IR of the samples LZ11, LS11, and ZS11 of lithium zirconate, lithium silicate, and zirconium silicate. **c** The IR of the samples LZS611, LZS411, LZS311, and LZS11 of lithium zirconate silicate

alkalinity 20.16, 21.89, 22.47 and 24.03 mmol g^{-1}, respectively. The results indicate that the alkalinity of the samples of lithium zirconium silicate was showing the increased trend with the increased lithium content. Thus, the addition of lithium in the zirconium silicate changes the acidity to alkalinity.

In Fig. 3, the SEM images of the samples LZS111, LZS311, LZS411, and LZS611 of lithium zirconium silicate with mole ratios Li/Zr/Si, 1:1:1, 3:1:1, 4:1:1, 6:1:1, were shown. The predominantly formed crystalline phases of lithium zirconate Li_2ZrO_3, Li_4ZrO_4, the phases of lithium silicate, Li_2SiO_3, Li_4SiO_4, and the phases of zirconium silicate $ZrSiO_4$ were observed in the samples LZS111, LZS311, LZS411, and LZS611 of lithium zirconium silicate with mole ratios Li/Zr/Si, 1:1:1, 3:1:1, 4:1:1, 6:1:1. The crystalline

Table 1 Alkalinity/acidity and surface area of the samples of the lithium zirconium silicate

Sr. no.	Lithium zirconium silicate Sample	Alkalinity/acidity (mmol g^{-1})	Surface area (m^2/g)
1	LZ61 (Li/Zr (6:1))	21.25	3.36
2	LS61 (Li/Si (6:1))	21.34	6.94
3	ZS11 (Zr/Si (1:1))	0.23 (Acidity)	98.71
4	LZS111 (Li/Zr/Si (1:1:1))	20.16	0.05
5	LZS311 (Li/Zr/Si (3:1:1))	21.89	0.16
6	LZS411 (Li/Zr/Si (4:1:1))	22.47	1.43
7	LZS611 (Li/Zr/Si (6:1:1))	24.03	2.13

Sr. no. serial number

phases of lithium zirconate Li_2ZrO_3, Li_4ZrO_4, lithium silicate Li_2SiO_3, Li_4SiO_4, and zirconium silicate $ZrSiO_4$ were observed with the particle showing the uniform crystal size pattern. The SEM images showed the particle size of the samples of the lithium zirconium silicate. However, the samples of lithium zirconium silicate had uniform particle size.

The changes in the morphology of the crystals were observed. The comparison in Fig. 3a, b, and d showed that the dominant growth of plate-like particles was observed instead of spherical particles in Fig. 3a. Even in Fig. 1b, the XRD peak position seems to be different from Fig. 1d. This suggests growth of different crystal structures (Fig. 1b, d). The observed results of the sample of lithium silicate showed that the particle size and morphology of the crystals were also changed (Figs. 1, 2, and 3).

In Fig. 4a, the weight loss of the sample LZS611 of lithium zirconium silicate against the temperature was shown. The results show that the there is a low weight loss in the sample. In Fig. 4b, the differential scanning calorimetric heat flow against temperature was shown for the sample LZS611 of lithium zirconium silicate. The heat flow started increasing at 300 °C and continues until the temperature reaches 800 °C. This indicated that the exothermic reaction has occurred. However, above 800 °C, the heat flow started decreasing. This showed the endothermic reaction. Thus, the thermal stability and heat capacity of sample LZS611 of lithium zirconium silicate was observed in Fig. 4b.

The ^{29}Si NMR of sample LZS611 of lithium zirconium silicate is shown in Fig. 4c. The results of ^{29}Si NMR showed that the chemical shift had been moved

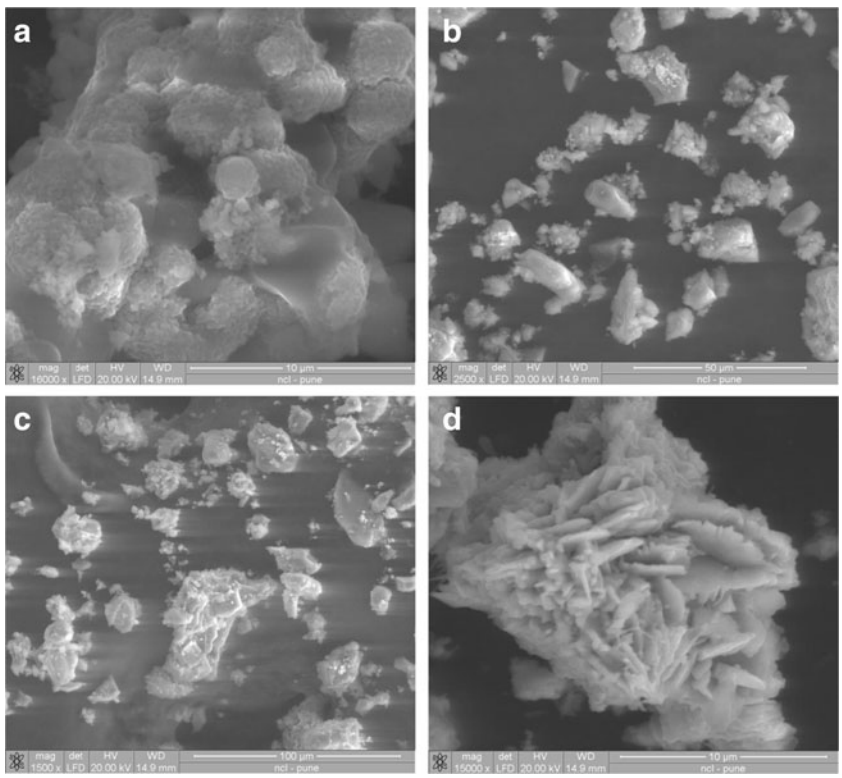

Fig. 3 The SEM images of the lithium zirconium silicate samples **a** LZS111 (Li/Zr/Si, 1:1:1), **b** LZS311 (Li/Zr/Si, 3:1:1), **c** LZS411 (Li/Zr/Si, 4:1:1), and **d** LZS611 (Li/Zr/Si, 6:1:1) were prepared by the solid–solid fusion method

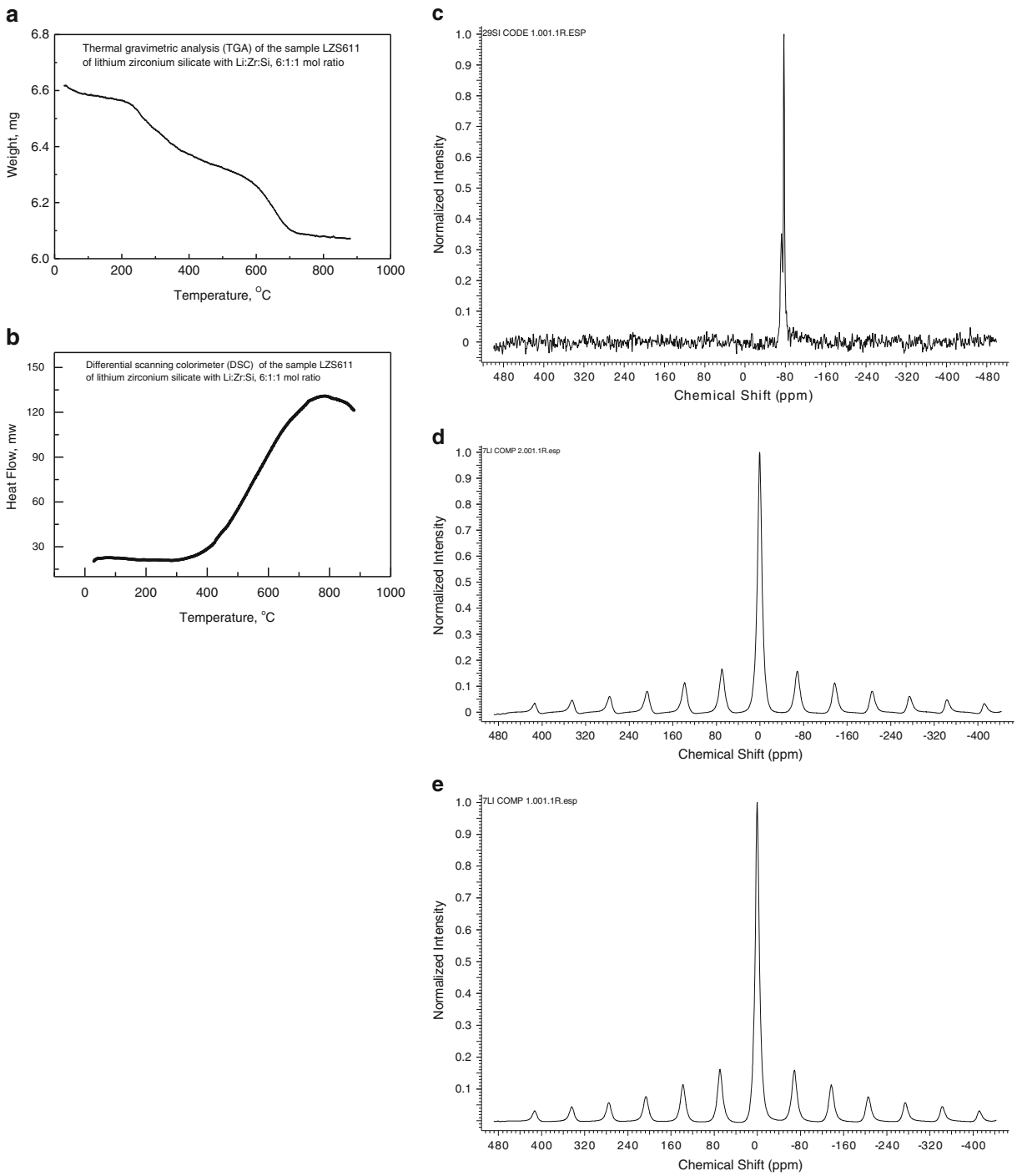

Fig. 4 **a** Thermal gravimetric analysis of lithium zirconium silicate sample LZS611 (Li/Zr/Si, 6:1:1). **b** Differential scanning calorimetric observations for the heat flow against temperature of the lithium zirconium silicate sample LZS611. **c** The ^{29}Si NMR of the sample LZS611 of lithium zirconium silicate. **d** The ^{7}Li NMR of the sample LS61 of lithium silicate. **e** The ^{7}Li NMR of the sample LZS611 of lithium zirconium silicate

toward −80 ppm. That indicated that the silicon is not tetrahedral bonded but multi-bonded. The ^{7}Li NMRs of samples LS61 of lithium silicate and sample LZS611 of lithium zirconium silicate showed the

signals at 12 places. The ^{7}Li NMR spectrum showed a large number of signals arising from the molecular complex materials.

3.2 The Effect of Li/Zr/Si Mole Ratio on the Carbon Dioxide Sorption by the Samples of Lithium Zirconium Silicate

The CO_2 captured by the different phases could be related to the enthalpy of formation of different phases (Wyers et al. 1989). The more enthalpy is required for the formation of crystalline phase, this indicates the CO_2 capture also required more enthalpy for the formation of carbonate. Therefore, the CO_2 captured by the different phases could be as in the increasing order of enthalpy, Li_2ZrO_3 (−1,742.8 kJ mol^{-1})<Li_4ZrO_4< $Li_6Zr_2O_7$ (−4,107.1 kJ mol^{-1})< Li_8ZrO_6 (−3,559.7 kJ mol^{-1}) (Wyers et al. 1989). These phases simultaneously more or less could be contributed to CO_2 capture. There were two peaks observed (Hutson and Attwood 2008). The first peak represented the physic-sorption of weakly bound CO_2. The second peak represented the chemisorptions of strongly bound CO_2. The observed results were given for the physic-sorption, chemisorptions, and combined.

The results of the CO_2 sorption with the different samples LZS111, LZS311, LZS411, and LZS611 of lithium zirconium silicates with mole ratios Li/Zr/Si, 1:1:1, 3:1:1, 4:1:1, 6:1:1 at 550 °C were given in Table 2. Sample LZS611 of lithium zirconium silicate with L/Zr/Si, 6:1:1 mole ratio was also calcinied in the nitrogen atmosphere in order to check the effect of neutral calcination atmosphere for the CO_2 adsorption by the sample of lithium zirconium silicate. The different samples LZS111, LZS311, LZS411, and LZS611 of lithium zirconium silicate with mole ratios Li/Zr/Si, 1:1:1, Li/Zr/Si, 3:1:1, Li/Zr/Si, 4:1:1, Li/Zr/Si, 6:1:1 were tested for the CO_2 adsorption at 300, 500, and 550 °C. Sample LZ61 of lithium silicate with Li/Zr, 6:1 mole ratio, sample LS61 of lithium silicate with Li/Si, 6:1 mole ratio, and sample ZS11 of zirconium silicate with Zr/Si, 1:1 mol ratios were tested for the CO_2 adsorption at 550 °C. The CO_2 adsorption was varied from 5.44 to 16.68 wt.%. The physic-sorption of CO_2 was low at 500 °C; however, the chemisorptions of CO_2 was higher. The physic-sorption of CO_2 was higher at 300 °C.

3.3 Temperature Profile for the Carbon Dioxide Sorption by the Sample of Lithium Zirconium Silicate

In Fig. 5, the temperature profile of CO_2 sorption by sample LZS611 of lithium zirconium silicate with mole ratio (Li/Zr/Si, 6:1:1) was presented for the temperature range from 100 to 700 °C. The data of the CO_2 sorption were presented in terms of physic-sorption, chemisorptions, and combined sorption. The observed CO_2 captured by the different phases

Table 2 The adsorption of CO_2 by the samples of the lithium zirconium silicate at the exposure temperature 550 °C, exposure time 25 min, and exposure pressure 30 psi

Sr. no.	Lithium zirconium silicate sample	CO_2 adsorption, wt.%		
		Physic-sorption	Chemisorptions	Combined
Calcined in air at 900 °C and CO_2 adsorption at 550 °C				
1	LZ61 (Li/Zr, 6:1)	Absent	14.87	14.87
2	LS61 (Li/Si, 6:1)	1.93	12.96	14.89
3	ZS11 (Zr/Si, 1:1)	5.44	Absent	5.44
4	LZS111 (Li/Zr/Si, 1:1:1)	3.94	7.85	11.79
5	LZS311 (Li/Zr/Si, 3:1:1)	2.61	11.32	13.93
6	LZS411 (Li/Zr/Si, 4:1:1)	2.57	12.15	14.72
7	LZS611 (Li/Zr/Si, 6:1:1)	1.19	15.49	16.68
Calcined in N_2 at 900 °C and CO_2 adsorption at 300 or 500 °C				
8	LZS611 (Li/Zr/Si, 6:1:1) at 300 °C	13.87	0.13	14.00
9	LZS611 (Li/Zr/Si, 6:1:1) at 500 °C	1.55	14.68	16.23

Sr. no. serial number

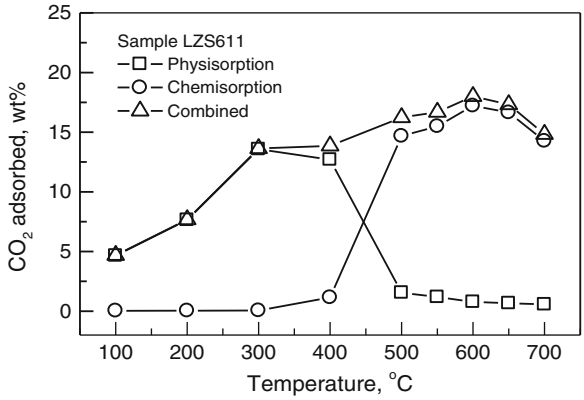

Fig. 5 Temperature profile of CO_2 sorption over lithium zirconium silicate sample LZS611 (Li/Zr/Si, 6:1:1)

of lithium zirconium silicate could be given by the enthalpy of formation of different phases (Wyers et al. 1989). For those phases, the carbonate formation could also depend on the enthalpy of carbonate formation. Phases $ZrSiO_4$, Li_2SiO_3, Li_2ZrO_3, Li_4ZrO_4, Li_4SiO_4, $Li_6Si_2O_7$, etc. could simultaneously, more or less, contribute to the CO_2 sorption. The enthalpies of the formation of different phases were observed as in the order Li_2ZrO_3 (−1,742.8 kJ mol^{-1})<Li_4ZrO_4<$Li_6Zr_2O_7$ (−4,107.1 kJ mol^{-1})<Li_8ZrO_6 (−3,559.7 kJ mol^{-1}) (Wyers et al. 1989). The phase $Li_6Si_2O_7$ of lithium zirconium silicate could relatively show the low CO_2 sorption in comparison with the other phases $ZrSiO_4$, Li_2SiO_3, Li_2ZrO_3, Li_4ZrO_4, and Li_4SiO_4 under same conditions at the lower temperature. The CO_2 sorption by the sample of lithium zirconium silicate was observed in two major temperature zones. The first CO_2 sorption zone was from 100 to 400 °C, where the physic-sorption was higher. The second CO_2 sorption zone was found from the 500 to 700 °C, where the chemisorptions were higher. The physic-sorption was in the range 0.57 to 13.57 wt.%. However, the chemisorptions were in the range 0.033 to 17.22 wt.%. In the first temperature, CO_2 sorption zone 100 to 400 °C, the CO_2 sorption by the sample of lithium zirconium silicate was 4.69 to 13.85 wt.%. However, in the second temperature zone, 500 to 700 °C, CO_2 sorption was 14.83 to 18 wt.%. The CO_2 sorption by the sample of lithium zirconium silicate was 14.83 wt.% at 700 °C. In the temperature range 500 to 700 °C, CO_2 sorption by the sample of lithium zirconium silicate showed the formation of lithium carbonate and released the silica and zirconia. The reversible reactions were also observed in this temperature zone. Therefore, lithium zirconium silicate mixed metal oxides are the regenerable adsorbent for CO_2.

3.4 Pressure Profile for the Carbon Dioxide Sorption by the Sample of the Lithium Zirconium Silicate

In Fig. 6, the effect of CO_2 pressure on the CO_2 sorption by sample LZS611 of lithium zirconium silicate with Li/Zr/Si, 6:1:1 mole ratio was shown in the range 10 to 30 psi. The data of the CO_2 sorption were presented in terms of physic-sorption, chemisorptions, and combined sorption. The captured CO_2 by the sample of lithium zirconium silicate was increased in both temperatures 300 and 500 °C with the increase in pressure from 10 to 30 psi. The physic-sorption was in the range 6.57 to 13.87 wt.% at 300 °C. However, the chemisorptions were 14.36 to 16.20 wt.% at 500 °C.

3.5 The Conversion of CO_2 by CH_4 to Syn-gas over Lithium Zirconium Silicate and Alumina-Supported Palladium

The conversion of CO_2 by methane to syn-gas was carried out over sample LZS611 of lithium zirconium silicate with Li/Zr/Si, 6:1:1 mole ratio at 500 °C. Among the gas hourly space velocities (GHSV) of CO_2, methane and helium, the GHSV of CO_2 and helium were kept constant at 6,000 mL h^{-1} g^{-1}; however, the GHSV of methane were varied from 6000, 12,000, and 36,000 mL h^{-1} g^{-1} (Fig. 7). The results of the conversion of CO_2 and CH_4 to syn-gas showed the increased conversion of CO_2 and methane at the low

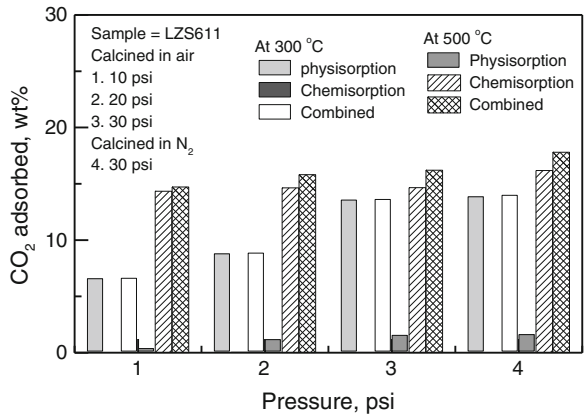

Fig. 6 Pressure profile of CO_2 sorption over lithium zirconium silicate sample LZS611 (Li/Zr/Si, 6:1:1) at the temperatures 300 and 500 °C

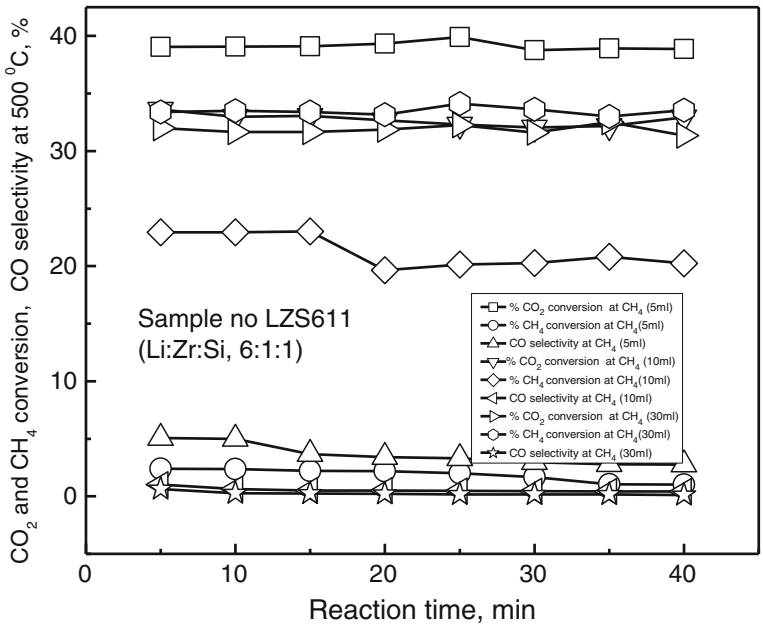

Fig. 7 The conversion of CO_2 by methane to syn-gas over the lithium zirconium silicate sample LZS611 (Li/Zr/Si, 6:1:1) at 500 °C

gas hourly space velocity of methane. However, the conversion of CO_2 and methane with the increase in gas hourly space velocity of methane showed the decrease in their values.

With the increase in gas hourly space velocity of methane (high mole ratio of methane) at the constant gas hourly space velocity of CO_2 (low mole ratio of CO_2), the selectivity of CO decreases with increasing the selectivity of H_2O and carbon (Eq. 9). Hence, at the low gas hourly space velocity of methane (low mole ratio of methane) and high gas hourly space velocity of CO_2 (high mole ratio of CO_2), the syn-gas formation favors Eq. 8.

$$CO_2(\text{at low mole ratio}) + CH_4(\text{at high mole ratio}) \leftrightarrow 2C + 2H_2O \quad (9)$$

The temperature effect shows that the CO selectivity is higher at 300 °C in comparison with that of at the 500 °C.

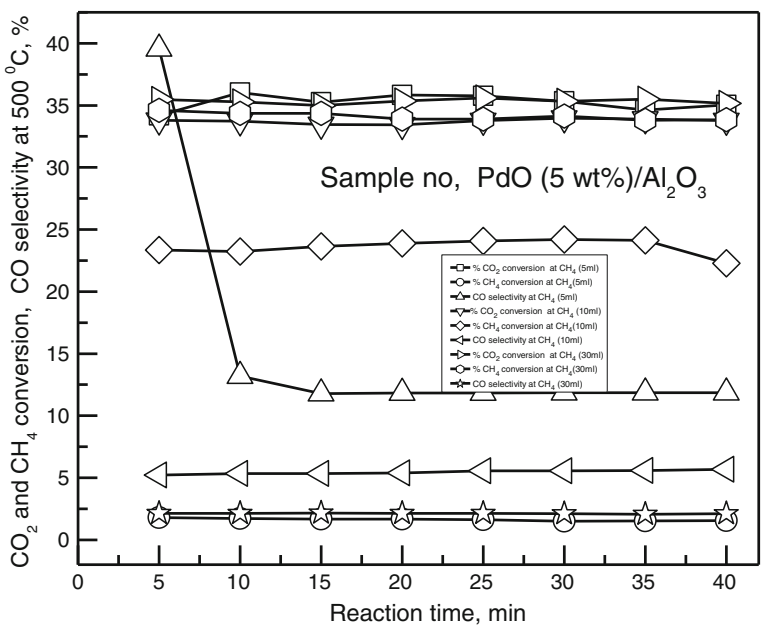

Fig. 8 The conversion of CO_2 by methane to syn-gas over the alumina-supported palladium oxide, PdO (5wt%)/Al_2O_3, at 500 °C

The conversion of CO_2 by methane was carried out over the alumina-supported palladium oxide, PdO (5 wt.%)/Al_2O_3, at 500 °C. Among the GHSV of CO_2, methane and helium, the GHSV CO_2 and helium were kept constant 6,000 mL h^{-1} g^{-1}; however, the GHSV of methane were varied from 6000, 12,000, and 36,000 mL h^{-1} g^{-1} (Fig. 8). The results of the conversion of CO_2 and CH_4 to syn-gas showed the increased conversion of CO_2 and methane at the low gas hourly space velocity of methane. However, the conversion of CO_2 and methane with the increase in gas hourly space velocity of methane showed the decrease in their values.

With the increase in the gas hourly space velocity of methane (high mole ratio of methane) at the constant gas hourly space velocity of CO_2 (low mole ratio of CO_2), the selectivity of CO decreases with the increase in selectivity of H_2O and carbon (Eq. 9). Hence, at the low gas hourly space velocity of methane (low mole ratio of methane) and high gas hourly space velocity of CO_2 (high mole ratio of CO_2) the syn-gas formation favors Eq. 8. However, PdO/Al_2O_3 catalyst at 500 °C shows the high selectivity to CO in comparison with that of sample LZS611 of the lithium zirconium silicate catalyst.

The studied mole ratios of CO_2/CH_4 for the conversion of CO_2 by CH_4 were $CO_2/CH_4=2$, $CO_2/CH_4=1$, and $CO_2/CH_4=0.33$. The conversions of CO_2 by CH_4 were noted as follows. The conversion of CO_2 by CH_4 depends on the CO_2/CH_4 mole ratio, when $CO_2/CH_4>1$ mole ratio, then, CO_2 by CH_4 is converted to syn-gas (oxidation process is favorable, where the CO_2 conversion is comparatively higher than that of CH_4). However, when, $CO_2/CH_4<1$ mole ratio, then CO_2 by CH_4 is converted into carbon and water (reduction process is favorable, where the CO_2 conversion is comparatively lower than that of CH_4). Thus, CO_2/CH_4 mole ratio is an important factor for achieving the desired product. When $CO_2/CH_4>1$ mole ratio, then, CO_2 conversion is higher in comparison with that of CH_4. Moreover, $CO_2/CH_4<1$ mole ratio, then CH_4 conversion is higher in comparison with that of CO_2. Thus, under extreme conditions of mole ratios of $CO_2/CH_4>>>1$, the oxygenated product of CH_4 and CO_2 could be possible. However, on the other hand, when mole ratios of $CO_2/CH_4<<<1$, then the hydrogenated product of CO_2 and methane could be possible.

4 Conclusions

In the mixed metal oxide systems, the important aspects explored were the contribution of mixed metal oxides for the CO_2 sorption and conversion to syn-gas. The different samples of lithium zirconium silicate were prepared by solid–solid fusion method. The samples of lithium zirconium silicate were characterized for alkalinity, surface area, XRD patterns, and SEM images. The alkalinity and CO_2 sorption of the samples of the lithium zirconium silicate increases with the increase in the Li/Zr/Si mole ratio of lithium in the samples of lithium zirconium silicate from 1 to 6. The conversion of CO_2 by methane over the sample of lithium zirconium silicate and alumina-supported palladium oxide at 500 °C produced the syn-gas. However, the observed syn-gas was higher at the lower gas hourly space velocity of methane. Thus, the CO_2 adsorbent could be used to produce syn-gas by the reaction of CO_2 and methane.

Acknowledgments The authors are grateful to the CSIR for the network project research grant NWP0021H

References

Avalos-Rendon, T., Casa-Madrid, J., & Pfeiffer, H. (2009). Thermo-chemical capture of carbon dioxide on lithium aluminates ($LiAlO_2$ and Li_5AlO_4): a new option for the CO_2 absorption, *Journal of Physical Chemistry, A, 113*(25), 6919–6923.

Bondioli, F., Manfredini, T., Siligardi, C., & Ferrari, A. M. (2004). A new glass–ceramic red pigment. *Journal of the European Ceramic Society, 24*(14), 3593–3601.

Centi, G., & Perathoner, S. (2010). Opportunities and prospects in the chemical recycling of carbon dioxide to fuels. *Catalysis Today, 148*, 191–205.

Chatti, R., Bansiwal, A. K., Thote, J. A., Kumar, V., Jadhav, P., Lokhande, S. K., et al. (2009). Amine loaded zeolites for carbon dioxide capture: amine loading and adsorption studies. *Microporous and Mesoporous Materials, 121*(1–3), 84–89.

Djinovi, P., Crnivec, I. G. O., Batista, J., Levec, J., & Pintar, A. (2011). Catalytic syngas production from greenhouse gasses—performance comparison of Ru-Al_2O_3 and Rh-CeO_2 catalysts. *Chemical Engineering and Processing, 50*, 1054–1062.

Dunn, P. J., Rouse, R. C., Cannon, B., & Nelen, J. A. (1977). Zektzerite: a new lithium sodium zirconium silicate related to tuhualite and the osumilite group. *American Mineraloy, 62*, 416–420.

Edwards, J. H., & Maitra, A. M. (1995). The chemistry of methane reforming with carbon dioxide and its current

and potential applications. *Fuel Processing Technology, 42*, 269–289.

El-Naggar, I. M., & Abou-Mesalam, M. M. (2006). Synthesis, characterization and ion exchange properties of lithium zirconium silicate as inorganic ion exchanger. *Arabian Journal of Nuclear Science and Application, 39*(1), 50–60.

Etheridge, D. M., Steele, L. P., Langenfelds, R. L., Francey, R. J., Barnola, J. M., & Morgan, V. I. (1996). Natural and anthropogenic changes in atmospheric CO_2 over the last 1,000 years from air in Antarctic ice and firn. *Journal of Geophysical Research, 101*, 4115–4128.

Fan, S. M., Abdullah, Z. A., & Bhatia, S. (2010). Utilization of greenhouse gases through carbon dioxide reforming of methane over Ni–Co/MgO–ZrO_2: preparation, characterization and activity studies. *Applied Catalysis B: Environmental, 100*, 365–377.

Fauth, D. J., Hoffman, J. S., Reasbeck, R. P., & Pennline, H. W. (2004). CO_2 scrubbing with novel lithium zirconate sorbents. *Preprints of the American Chemical Society Division of Fuel Chemistry, (SAUS), 49*(1), 310–311.

Fauth, D. J., Frommell, E. A., Hoffman, J. S., Reasbeck, R. P., & Pennline, H. W. (2005). Eutetic salt promoted lithium zirconate: novel high temperature sorbent for CO_2 capture. *Fuel Processing Technology, 86*, 1503–1521.

Gao, W., Zhao, Y., Liu, J., Huang, Q., He, S., Li, C., et al. (2013). Catalytic conversion of syngas to mixed alcohols over CuFe-based catalysts derived from layered double hydroxides. *Catalysis Science and. Technology.* doi:10.1039/C3CY00025G.

Graves, C., Ebbesen, S. D., Mogensen, M., & Lackner, K. S. (2011). Sustainable hydrocarbon fuels by recycling CO_2 and H_2O with renewable or nuclear energy. *Renewable and Sustainable Energy Reviews, 15*, 1–23.

Gupta, H., & Fan, L. S. (2002). Carbonation-calcination cycle using high reactivity calcium oxide for carbon dioxide separation from flue gas. *Industrial and Engineering Chemistry Research, 41*, 4035–4042.

Hellstrom, E. E., & Van Gool, W. (1981). Li ion conduction in Li_2ZrO_3, Li_4ZrO_4 and $LiScO_2$. *Solid State Ionics, 2*, 59–64.

Hutson, N. D., & Attwood, B. C. (2008). High-temperature adsorption of CO_2 on various hydrotalcite-like compounds. *Adsorption, 14*(6), 781–789.

Ida, J. I., & Lin, Y. S. (2003). Mechanism of high-temperature CO_2 sorption on lithium zirconate. *Environmental Science and Technology, 37*(9), 1999–2004.

Ide, J. I., Xiong, R., & Lin, Y. S. (2005). Synthesis and CO_2 sorption properties of pure and modified lithium zirconate. *Separation and Purification Technology, 36*(1), 41–51.

Iwan, A., Stephenson, H., Ketchie, W. C., & Lapkin, A. A. (2009). High temperature sequestration of CO_2 using lithium zirconates. *Chemical Engineering Journal, 146*(2), 249–258.

Kaiser, A., Lobert, M., & Telle, R. (2008). Thermal stability of zircon ($ZrSiO_4$). *Journal of the European Ceramic Society, 28*, 2199–2221.

Kalinkin, A. M., Boldyrev, V. V., Politov, A. A., Kalinkina, E. V., Makaraov, V. N., & Kalinnkov, V. T. (2003). Investigation into the mechanism of interaction of calcium and magnesium silicates with carbon dioxide in the course of mechanical activation. *Glass Physics and Chemistry, 29*(4), 410–414.

Khomane, R. B., Sharma, B. K., Saha, S., & Kulkarni, B. D. (2006). Reverse micro emulsion mediated **sol–gel** synthesis of lithium silicate nanoparticles under ambient conditions: scope for CO_2 sequestration. *Chemical Engineering Science, 61*(4), 3415–3418.

Minghua, W., Choong-Gon, L., & Chong-Kul, R. (2008). CO_2 sorption and desorption efficiency of Ca_2SiO_4. *International Journal of Hydrogen Energy, 33*, 6368–6372.

Nakagawa, K., Kato, M., Yoshikawa, S., Essaki, K., Uemoto, H. (2003). *Second annual conference on carbon sequestration, May 5–8*. Hilton Alexandria mark centre Alexandria, VA.

NOAA National Climatic Data Center (2012). State of the climate: global analysis for November 2012. http://www.ncdc.noaa.gov/sotc/global/. Accessed 17 December 2012

Nikoo, K. M., & Amin, N. A. S. (2011). Thermodynamic analysis of carbon dioxide reforming of methane in view of solid carbon formation. *Fuel Processing Technology, 92*, 678–691.

Ochoa-Fernandez, E., Ronning, M., Grande, T., & Chen, D. (2006a). Nanocrystalline lithium zirconate with improved kinetics for high-temperature CO_2 capture. *Chemistry Material, 18*(6), 1383–1385.

Ochoa-Fernandez, E., Ronning, M., Grande, T., & Chen, D. (2006b). Synthesis and CO_2 capture properties of nanocrystalline lithium zirconate. *Chemistry Material, 18*(6), 6037–6046.

Pen, M. A., Gomez, J. P., & Fierro, J. L. G. (1996). New catalytic routes for syngas and hydrogen production. *Applied Catalysis A: General, 144*(2), 7–57.

Pfeiffer, H., & Bosch, P. (2005). Thermal stability and high-temperature carbon dioxide sorption on hexa-lithium zirconate ($Li_6Zr_2O_7$). *Chemistry Material, 17*(7), 1704–1710.

Pfeiffer, H., Vázquez, C., Lara, V. H., & Bosch, P. (2007). Thermal behavior and CO_2 absorption of $Li_{2-x}Na_xZrO_3$ solid solutions. *Chemistry Material, 19*(4), 922–926.

Stuckert, N. R., & Yang, R. T. (2011). CO_2 capture from the atmosphere and simultaneous concentration using zeolites and amine-grafted SBA-15. *Environmental Science and Technology, 45*(23), 10257–10264.

Venegas, M. J., Fregoso-Israel, E., Escamilla, R., & Pfeiffer, H. (2007). Kinetic and reaction mechanism of CO2 sorption on Li4SiO4: study of the particle size effect. *Industrial and Engineering Chemistry Research, 46*, 2407–2412.

Wang, M., & Lee, C. G. (2009). Absorption of CO_2 on $CaSiO_3$ at high temperatures. *Energy Conversion and Manangement, 50*(3), 636–638.

Wyers, G. P., Cordfunke, E. H. P., & AOuweltjes, W. (1989). The standard molar enthalpies of formation of the lithium zirconates. *The Journal of Chemical Thermodynamics, 21*, 1093–1100.

Yi, K. B., & Eriksen, D. O. (2006). Low temperature liquid state synthesis of lithium zirconate and its characteristics as a CO_2 sorbent. *Separation Science and Technology, 41*, 283–296.

Yin, H., Mao, X., Tang, D., Xiao, W., Xing, L., Zhu, H., Wang, D., Sadoway, D.R. (2013) Capture and electrochemical conversion of CO_2 to value-added carbon and oxygen by molten salt electrolysis. *Energy and Environmental Science*, 2013. doi:10.1039/C3EE24132G

Yong, Z., Mata, V., & Rodriguez, A. E. (2001). Adsorption of carbon dioxide onto hydrotalcite-like compounds (HTlcs) at high temperatures. *Industrial and Engineering Chemistry Research, 40*(1), 204–209.

Zhang, A., Zhu, A., Guo, J., Xu, Y., & Shi, C. (2010). Conversion of greenhouse gases into syngas via combined effects of discharge activation and catalysis. *Chemical Engineering Journal, 156*, 601–606.